European Journal of Neuroscience, Vol. 16, pp. 1994–2000, 2002

Object-based visual neglect: a computational hypothesis

Gustavo Deco[1] and Edmund T. Rolls[2]
[1]Siemens AG, Corporate Technology, Computational Neuroscience, CT IC 4, D-81730 Munich, Germany
[2]University of Oxford, Department of Experimental Psychology, South Parks Road, Oxford OX1 3UD, UK

Keywords: attention, inferior temporal visual cortex, neglect, parietal cortex

Abstract

Some patients with damage to the right parietal cortex show neglect for the left half of each of a series of objects shown in a horizontal row in the visual field. The neglect is thus not based on failure to see objects in any part of left visual space, but is object-based. We show that in a model of attention with separate V1, object (inferior temporal cortex, IT) and spatial (posterior parietal cortex, PP) modules the effect can arise after graded damage increasing towards the right of the PP module when the lateral inhibition between neurons in the PP and V1 modules is short-range. The local lateral inhibition produces high contrast effects at the edges of each object, and it is when this interacts with gradually increasing damage through the left visual field that the visibility of the left half of each object is especially impaired. This result was found in a formal model completely specified by mean field equations to quantify the dynamical interactions between the modules. This is the first quantitative account of object-based neglect found in humans with right parietal cortex damage, and provides evidence that the model of attention we describe can account for even detailed and extraordinary phenomena that can occur in visual perception.

Introduction

Damage to the right parietal cortex of humans can produce a neglect of the left half of visual space, which is called hemineglect. The effect is especially evident when two objects are present in the visual fields, when the object in the right visual field is seen and the object in the left visual field is not seen or is neglected. The effect is not just blindness to any object in the left visual field (which can occur after damage in the early visual pathways, e.g. in the geniculo-striate projection) for, in left hemineglect produced by right parietal cortex damage, an object can be seen in the left visual hemifield if there is no object in the right visual field. [Although visual neglect can be present in the left or right hemispace, we refer in the following to left-sided visual neglect (produced by damage to the right parietal cortex), because this type is more frequently observed (Vallar & Pernai, 1986)]. The effect for which we provide an account in this report is a more extraordinary type of neglect in which the left half of each of a series of objects spread out horizontally in the visual field is not seen or 'neglected' (Marshall & Halligan, 1993; Gilchrist *et al*., 1996). Because this effect occurs separately for the left half of each object, it cannot be accounted for just by neglect of the left half of visual space. The impairment is called object-based visual neglect because the neglect is with respect to each object, and not to the visual field. In this paper we show that object-based neglect arises in a model of attention if the lateral inhibition operates over only a short range.

Theoretical models of visual neglect can usually be divided into approaches based on a representational or on an attentional account of the syndrome (Humphreys & Heinke, 1998; Driver *et al*., 1994; Bisiach, 1996; Pouget & Driver, 1999). A representational account interprets neglect as the result of impairment of one side of a particular spatial representation, whereas an attentional account considers neglect as a deficit in orienting visual attention to the affected hemispace. The attentional account is strongly favoured by two types of evidence: first, the asymmetrical effect of spatial cueing on neglect (Rafal & Robertson, 1997; Posner *et al*., 1984) and, second, the phenomenon of extinction in the framework of visual search (Eglin *et al*., 1989). In both cases, the degree of impairment increases when the stimulus on the affected side has to compete with a second stimulus at the unaffected side, relative to the condition when only one stimulus is on the affected side. This kind of asymmetry is consistent with the idea that the stimulus in the neglected field attracts attention only in a weak way. Driver & Pouget (2000) describe an attempt to reduce object-centred neglect to relative egocentric neglect.

Deco (2001) has developed a model of attention that can account for visual hemineglect including the above phenomena (see also Rolls & Deco, 2002; Deco *et al*., 2002). In this paper we develop the model further by incorporating local lateral inhibition (instead of global inhibition) within modules that simulate the posterior parietal cortex (PP) and the primary visual cortex, V1, and show that this enables us to account for object-based neglect in which the left half of each of a row of objects is neglected. Our account of visual neglect is based on damage to the posterior parietal module, which is the module representing and controlling the spatial location of visual attention. We describe the general architecture of the model next, and how damage to it can produce object-based neglect. The model is implemented by mean-field equations to describe the interactions between the modules. The equations for the model, which specify it completely, are provided in the Appendix.

Methods

The model

A simple version of the model with just three modules is able to capture the mechanisms that can account for object-based neglect. The model is shown in Fig. 1, and is defined quantitatively in the

Correspondence: Professor Edmund T. Rolls, as above.
Email: Edmund.Rolls@psy.ox.ac.uk

Received 9 July 2002, revised 30 August 2002, accepted 4 September 2002

doi:10.1046/j.1460-9568.2002.02279.x

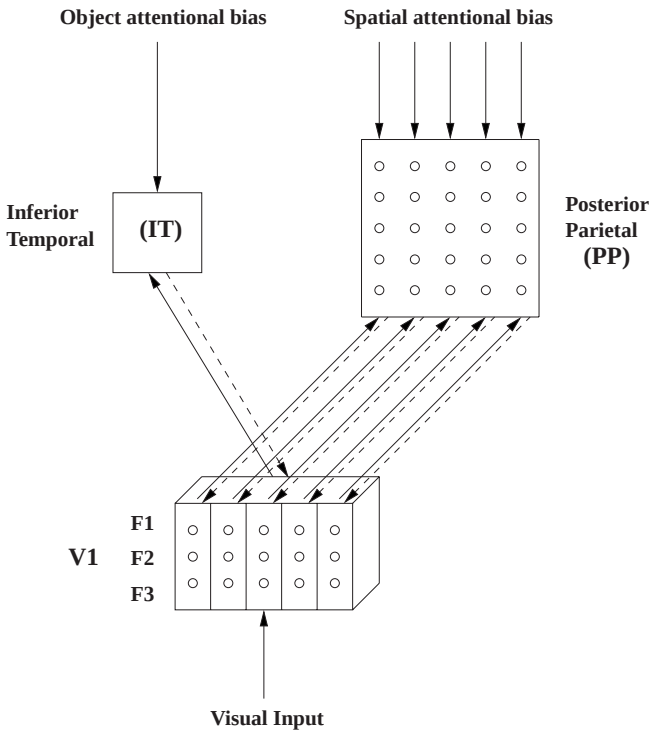

FIG. 1. The trimodular architecture of the model, which includes a V1 (primary visual cortex) module, a posterior parietal cortex (PP) module in a dorsal visual stream and an inferior temporal cortex (IT) module in the ventral visual stream. The V1 and PP modules have spatial topology. In V1, different shape feature descriptors are present, labelled F1, F2 etc, which in the model are Gabor wavelets with receptive fields like those of V1 simple cells. The model is defined quantitatively in the Appendix.

Appendix. There is a topologically organized V1 module, a topologically organized posterior parietal cortex (PP) module to represent the dorsal visual stream, and an inferior temporal cortex (IT) module to represent the ventral visual stream in which different neurons represent different objects and there is no spatial topology. There are reciprocal connections (feedforward and backprojections) between the VI and IT, and the V1 and PP modules. There is spatially local lateral inhibition in the V1 and PP modules, and global inhibition (i.e. acting across all neurons) in the IT module. Images of spatial scenes are presented to the network via a set of Gabor filters with three spatial frequencies and eight orientations which produce firing similar to that of simple cells in V1. The reciprocal connections between V1 and IT are trained by an associative (Hebb-like) synaptic training rule in which an image with an object at one position in a scene is presented to V1, and the neurons in IT that code for that object are set to be active. This procedure is repeated for different objects at different locations in the scene. The reciprocal connections between the V1 and PP modules are set so that corresponding positions in these two modules with spatial topology are connected, and nearby positions are less strongly connected according to a Gaussian spatial function. (This connectivity could in principle be set by associative learning, with self-organizing map formation also involved; see Rolls & Treves, 1998; Rolls & Deco, 2002). The IT module can receive an object bias which can be applied to neurons representing individual objects and can be used to bias attention towards particular objects, and the PP module can receive a spatial bias that can be applied to particular locations and can be used to bias attention towards particular locations (see Fig. 1).

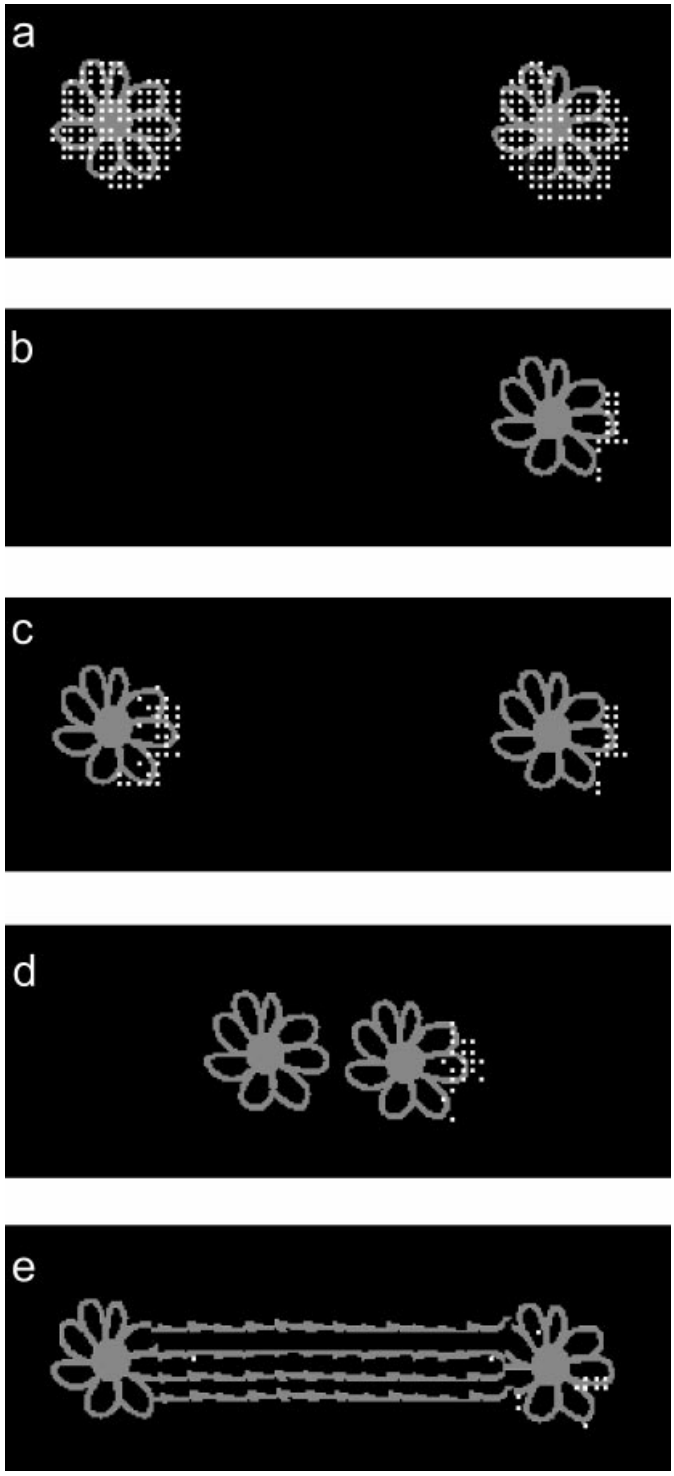

FIG. 2. (a–e) The locations in which activity in the PP module exceeded the threshold after the network had settled with each stimulus are shown by spots. (a) The operation of the unlesioned network; (b–e) the operation of the lesioned network (see text).

With this architecture, search for a target object can be produced by a spatial bias applied to the PP module. This bias moves what might be thought of as a spotlight of attention to a particular location in PP. The spatially organized top-down projections to V1 result in some facilitation of features at that location in the image being

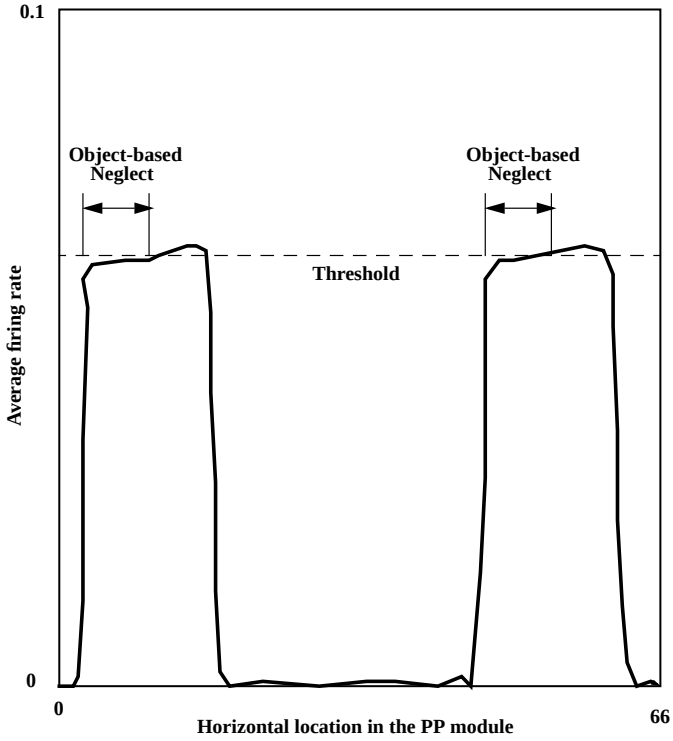

FIG. 3. The average firing rate of each of the neuronal pools at different horizontal positions in the posterior parietal (PP) module when the stimuli presented are as shown in Fig. 2b. The two regions of high firing correspond to the two flowers in Fig. 2b, and the short-range lateral inhibition superimposed on the lesion effect, which increases in severity towards the left of the Figure, produces a region of high firing at the right of each flower and a region of lower firing at the left of each flower.

presented to V1, and the facilitation of these features results in the correct object neurons in IT being activated as the whole network settles dynamically. In a corresponding way, search for the spatial location of an object can be produced by an object bias applied to the IT module. The object bias facilitates the firing of neurons representing that object in IT, and then the backprojections to V1 facilitate the firing of features found in those objects in the V1 representation. Where those features are present in the visual scene there will be enhanced firing in V1 neurons [because of the supporting top-down (attentional) and bottom up (visual) inputs], and the excess firing at those V1 locations will lead to the spatially corresponding locations in the PP module being activated. In this way the 'spotlight of attention' will move to the correct location in V1 where the searched-for object is present, as the network settles dynamically into its lowest energy state which optimally satisfies the constraints. This model can account in this way for object search, for spatial search, and even for so-called serial search when there are many distractors in a display, which is accounted for in the model by the longer time it takes for the model to settle in a totally parallel way into the energy minimum that best satisfies the constraints being applied (see Rolls & Deco, 2002).

Experimental design

To investigate object neglect in the new version of the model described here which introduces local lateral inhibition into the PP and V1 modules, we trained the network on the image shown in Fig. 2b at all possible locations on the retina. The PP module was then lesioned to model the gradient of impairment in neglect following right parietal cortex damage (Mozer & Behrmann, 1990; Kinsbourne, 1993; Driver *et al*., 1994; Anderson, 1996; Pouget & Sejnowski, 1997). In patients with right parietal cortex damage the response to stimuli is increasingly impaired the further the stimuli are towards the patient's (egocentric) left. The lesion accordingly consisted of damage that increased linearly from the left to the right in the PP module, producing an impairment in visual space that gradually increased from the right towards the left part of visual space. The lesion consisted of reducing the excitatory and other interactions within a pool of PP neurons according to the amount of the lesion (see Appendix, Equation 16). One or more examples of the visual stimulus (a flower) on which the network had been trained were then presented to the network. (No object or spatial attentional bias was used in the simulations described here.) The network was then allowed to settle dynamically, to find which locations the PP module settled on, and thus where 'attention' was being paid to in the visual scene, and which parts of the visual scene were being neglected.

Results

We performed the simulations without training the backprojection connections from IT to V1, in order to take into account only purely bottom-up attentional effects. Rolls & Deco (2002) and Deco *et al*. (2002) provide analyses of the effects of learning and top-down object-based attentional effects on visual neglect. The results of four different experiments are shown in Fig. 2b–e. In Fig. 2a the performance of the unlesioned model for the case of two objects (two flowers) is provided as the reference condition. The locations where in separate runs of the experiment the 'spotlight of attention' in the parietal module settled are shown as spots on the diagram. (Spots are placed on the diagram for spatial locations at which the activity of a PP neuronal pool was higher than a threshold. In the simulations described, the threshold was set at 0.0638. Each diagram shows the results of a single run of the simulation, and thus all neuronal pools that were above the threshold are shown in the diagram. The results on different simulation runs were very similar.) In the unlesioned condition shown in Fig. 2a the locations of the 'spotlight' were distributed onto the whole of both objects, indicating no neglect. In Fig. 2b a single object was presented in the right (more intact) part of visual space. The locations of the 'spotlight' were in the right half of the flower, and the left half of the object was neglected. Figure 2c shows two objects well separated in the right and the left of the display. The left half of each object is neglected. The right-hand part of the left object is 'seen', even though it is to the left of the right object. Thus the neglect is object-based, and not based on a neglect of the left half of egocentric space. This is the phenomenon of object neglect that is to be accounted for.

The deficit can be understood, with the help of the model, to arise because local spatial differentiation produced by the local lateral inhibition in the PP and V1 modules, superimposed on the linearly increasing deficit towards the left of visual space, results in some sparing of the right parts of each object wherever they are in the visual scene. The result of this combination of factors (for the stimulus conditions shown in Fig. 2c) is shown in Fig. 3. This shows the average firing rate of each of the neuronal pools at different horizontal positions in the PP module. The two regions of high firing correspond to the two flowers in Fig. 2c, and the short-range lateral inhibition superimposed on the lesion effect, which increases in severity towards the left of the figure, produces a region of high firing

at the right of each flower and a region of lower firing at the left of each flower. With the threshold set where shown to reflect where there is strongest firing in the PP module, and thus where attention is preferentially located, spotlights of attention are located on the right side of each object and the left half of each object is neglected.

The model, and the resulting understanding, allow us to predict and explain a number of further phenomena that can arise with neglect (Marshall & Halligan, 1993; Gilchrist *et al*., 1996). One is shown in Fig. 2d, in which two objects are placed close together in the scene. In this case the left part of the right object, and the whole of the left object, are neglected. This can be understood to arise because the local spatial differentiation produced by the local lateral inhibition in the PP and V1 modules now operates to produce enhancement only on the right of the object complex, because of the lateral scale of the lateral inhibition relative to the separation of the objects.

Another phenomenon predicted and explained by the model is illustrated in Fig. 2e. If the two objects, though widely separated, are joined by lines, then only the right object is seen, but not the left (Gilchrist *et al*., 1996). This is again accounted for by the local lateral inhibition which, when convolved with the whole object, results in an enhanced positive edge only at the right of the combined object after superimposition on the lesion effect which increases linearly towards the left of the visual field.

Discussion

This model produces the first account we know of object-based neglect. The model also predicts and accounts for the two effects shown in Fig. 2d and e.

The new aspect of the model that enables it to account for object-based neglect is the spatially local lateral inhibition implemented in the PP and V1 modules. It is this local lateral inhibition that when convolved with the objects present in the image and, combined with the damage in the processing that increases linearly towards the left of the visual field, produces local peaks in the resulting neuronal activation that enable for example the right half of an object to be seen when it is well to the left of another object in the scene (Fig. 2c).

The results described here provide a further example of the utility of the model of spatial and object search and attention that we have described (Deco, 2001; Rolls & Deco, 2002), and more generally for the utility of the computational neuroscience approach in helping to understand brain function.

The effects that we describe here must not be confused with the grouping effects observed in neglect (see for example Vuilleumier & Sagiv, 2001; Boutsen & Humphreys, 2002; Behrmann & Tipper, 1999). These papers suggest that grouping of contralateral items with ipsilateral ones, at both perceptual and semantic levels, reduces neglect and extinction. In this paper, we are only interested in explicitly modelling the competition effects resulting from local inhibitory connections in neglect, and are not concerned with perceptual grouping in neglect. Of course, perceptual grouping effects could also be explicitly included in the computational model. Indeed, we hypothesize that it is possible to implement the neural substrate of grouping by excitatory lateral connections (probably in V1, V2) in such a way that the lateral excitatory connections express certain Gestalt Grouping rules. These bottom-up cooperative mechanisms complement the competitive mechanisms on which our computational cortical model is based. Of course these excitatory cooperative interactions would then ameliorate neglect if grouping were present, in the ways described in the literature. However, we emphasize that the effect that we consider is not grouping but, instead, the local competition that can produce the object-based neglect shown in Fig. 2c.

Let us conclude with a final remark. As shown by Gainotti *et al*. (1972), object-centred neglect can appear in combination with page-centred neglect when genuinely complex scenes are copied. That is, on the right of the page there may be clear object-centred neglect whereas, at the more extreme left positions, items are omitted in their entirety. The computational model described here can account for such types of neglect by using different gradients of damage to the different parts of the system. For example, the combination of object-centred with page-centred neglect just described can be accounted for by pure damage (i.e. the lesion factor is constant with respect to angle in the visual field) in one hemisphere, together with a gradient of damage in the other. This could produce object-centred neglect in the contralateral hemifield related to the hemisphere with a gradient of damage, and a total page-centred neglect in the other hemifield related to the hemisphere with pure damage.

Appendix: definition and neurodynamic equations of the model

A model of brain functions requires the choice of an appropriate theoretical framework, which permits the investigation and simulation of large-scale biologically realistic neural networks. The model we describe is formulated using the mean-field approach because of its tractability. Starting from individual spiking neurons, one can derive a differential equation that describes the dynamic evolution of the averaged activity of a pool of a large number of similar neurons. The activity level of each pool of neurons, rather than the spiking activity of individual neurons, is used as the relevant dependent variable. It is possible to derive dynamical equations for the activity levels of a neuronal pool by utilizing the mean-field approximation (Wilson & Cowan, 1972; Abbott, 1991; Amit & Tsodyks, 1991). The mean-field approximation consists of replacing the temporally averaged discharge rate of a cell with an equivalent momentary activity of a neural population (the ensemble average) that corresponds to the assumption of ergodicity. According to this approximation, we categorize each cell assembly by means of its activity $A(t)$. A pool of excitatory neurons without external input can be described by the dynamics of the neuronal pool activity given by

$$\tau \frac{\partial A(t)}{\partial t} = -A(t) + q\mathrm{F}(A(t)) \qquad (1)$$

where the first term on the right hand side is a decay term and the second term takes into account the excitatory stimulation between the neurons in the pool. In the previous equation, the nonlinearity

$$\mathrm{F}(x) = \frac{1}{T_r - \tau \log(1 - \frac{1}{\tau x})} \qquad (2)$$

is the activation or response function (transforming the current x into discharge rate) for a spiking neuron with deterministic input, membrane time constant τ and absolute refractory time T_r. Equation 1 was derived by Gerstner (2000) assuming adiabatic conditions (i.e. the activity changes only slowly compared with the typical interval length).

The model

We now present a formal description of the model. We consider a pixelized grey-scale image given by an $N \times N$ matrix $\Gamma_{ij}^{\text{orig}}$. The subindices *ij* denote the spatial position of the pixel. Each pixel value is given a grey level brightness value coded in a scale between 0 (black) and 255 (white). We consider a retina of 66 × 66 pixels (i.e. $N = 66$). Feedforward connections to the layer of V1 neurons in the model perform the extraction of simple features like bars at different locations, orientations and sizes. Realistic receptive fields for V1 neurons that extract these simple features can be represented by 2D-Gabor wavelets, and we perform this preprocessing as described below to produce V1 feature-sensitive neurons with three spatial frequencies and eight orientations for each retinal pixel position, as described below. The V1 module contains therefore $66 \times 66 \times 8 \times 3$ neurons.

The wavelet preprocessing produces an input current in the V1 neurons. Let us denote by I_{pqkl}^{V1} the sensory input activity to a neuronal pool A_{pqkl}^{V1} in V1 which is sensitive to a spatial frequency at octave *k*, to a preferred orientation defined by the rotation index *l*, and to stimuli at the centre location in the cortical representation specified by the indices *pq*.

Let us denote by A_c^{IT} the activity of pool *c* in module IT. Similarly, let us denote with A_{ij}^{PP} the activity of a pool in the PP module corresponding to the location in the visual field. (The PP module contains 66×66 neurons.) The neurodynamical equations that regulate the temporal evolution of the whole system are given by the following set of coupled differential equations (in which $I^{\text{V1–IT}}$ denotes an input current to a V1 pool from the IT module, and the I^{I} terms reflect the operation of inhibitory neuronal pools defined below).

$$\tau \frac{\partial A_{pqkl}^{\text{V1}}(t)}{\partial t} = -A_{pqkl}^{\text{V1}} + \alpha \text{F}(A_{pqkl}^{\text{V1}}(t)) - \beta I_{pq}^{\text{I,V1}}(t) + I_{pqkl}^{\text{V1}}(t) + \gamma_b I_{pq}^{\text{V1–PP}}(t) + \lambda_b I_{pqkl}^{\text{V1–IT}}(t) + I_0 + \nu \quad (3)$$

$$\tau \frac{\partial A_c^{\text{IT}}(t)}{\partial t} = -A_c^{\text{IT}} + \alpha \text{F}(A_c^{\text{IT}}(t)) - \beta I^{\text{I,IT}}(t) + \lambda_f I_c^{\text{IT–V1}}(t) + I_0 + \nu \quad (4)$$

$$\tau \frac{\partial A_{ij}^{\text{PP}}(t)}{\partial t} = -A_{ij}^{\text{PP}} + \alpha \text{F}(A_{ij}^{\text{PP}}(t)) - \beta I_{ij}^{\text{I,PP}}(t) + \gamma_f I_{ij}^{\text{PP–V1}}(t) + I_0 + \nu \quad (5)$$

The spatial attentional biasing couplings $I_{pq}^{\text{V1–PP}}$ due to the intermodular 'where' connections with the pools in the parietal module PP are given by

$$I_{pq}^{\text{V1–PP}} = \sum_{i,j} \omega_{pqij}^{\text{V1–PP}} \text{F}(A_{ij}^{\text{PP}}(t)) \quad (6)$$

$$I_{ij}^{\text{PP–V1}} = \sum_{\tilde{p},\tilde{q},\tilde{k},\tilde{l}} \omega_{\tilde{p}\tilde{q}ij}^{\text{PP–V1}} \text{F}(A_{\tilde{p}\tilde{q}\tilde{k}\tilde{l}}^{\text{V1}}(t)) \quad (7)$$

The connections between pools in the V1 module and pools in the PP module are specified such that topographically corresponding centres (in PP and V1) are connected with maximal strength and the connections to neighbouring pools decay with a Gaussian function of distance. The mutual (i.e. forward and backprojection) connections between a pool A_{pqkl}^{V1} in V1 and a pool A_{ij}^{PP} in PP are therefore defined by

$$w_{pqij}^{\text{V1–PP}} = A \exp\left\{ -\frac{\text{dist}(c_{pq}, c_{ij})^2}{2\sigma_{\text{v1}}^2} \right\} \quad (8)$$

where c_{ab} corresponds to the 2D-centre in pixel retinal coordinates associated with the pool with space indices *ab* (in the V1 or PP module), and dist(c_1,c_2)is the Euclidean distance between centres c_1 and c_2. These connections mean that the V1 pool A_{pqkl}^{V1} will have maximal amplitude when spatial attention is located at c_{pq} in the visual field, i.e. when the pool A_{ij}^{PP} in PP corresponding to $c_{ij} = c_{pq}$ is maximally activated. In our simulations, we always used $A = 1$.

The feature-based attentional top-down biasing terms $A_{pqkl}^{\text{V1–IT}}$ due to the intermodular 'what' connections of pools between V1 and IT in the ventral stream are defined by

$$I_{kpql}^{\text{V1–IT}} = \sum_{c=1}^{C} w_{ckpql}^{\text{V1–IT}} \text{F}(A_c^{\text{IT}}(t)) \quad (9)$$

ω_{ckpql} being the connection strength between the V1 pool A_{kpql}^{V1} and the IT pool A_c^{IT} corresponding to the coding of a specific object category *c*. We assume that the IT module *C* has pools corresponding to different object categories. Similarly, the intermodular attentional biasing $I_c^{\text{IT–V1}}$ between IT and V1 pools is

$$I_c^{\text{IT–V1}} = \sum_{k,p,q,l} w_{ckpql}^{\text{IT–V1}} \text{F}(A_{kpql}^{\text{V1}}(t)) \quad (10)$$

The local lateral inhibitory interactions $I_{pq}^{\text{I,V1}}$ and $I_{pq}^{\text{I,IT}}$ in modules in the ventral stream are given by

$$I_{pq}^{\text{I,V1}} = \sum_{\tilde{p},\tilde{q},\tilde{k},\tilde{l}} w_{pq\tilde{p}\tilde{q}}^{\text{I,V1}} \text{F}(A_{\tilde{p}\tilde{q}\tilde{k}\tilde{l}}^{\text{V1}}(t)) \quad (11)$$

$$I_{pq}^{\text{I,IT}} = \sum_{\tilde{p},\tilde{q},\tilde{l}} w_{pq\tilde{p}\tilde{q}}^{\text{I,IT}} \text{F}(A_{\tilde{p}\tilde{q}\tilde{l}}^{\text{IT}}(t)) \quad (12)$$

In the preceding two equations $w_{pq\tilde{p}\tilde{q}}^{\text{I,VE}}$ denotes the lateral local connections between nodes within a layer defined by:

$$\begin{cases} w_{pq\tilde{p}\tilde{q}}^{\text{I,VE}} = 1.0 & \text{if } p = \tilde{p} \text{ and } q = \tilde{q} \\ w_{pq\tilde{p}\tilde{q}}^{\text{I,VE}} = -\delta \exp\left\{ -\dfrac{\text{dist}(c_{pq}, c_{\tilde{p}\tilde{q}})^2}{\sigma_{\text{VE}}^2} \right\} & \text{else} \end{cases} \quad (13)$$

where δ and σ control the amount and spread of lateral inhibition, respectively. Note that each cell is self excitatory ($w_{pq\tilde{p}\tilde{q}}^{\text{I,VE}} = 1$).

An important point in this paper is that we use a σ that is small enough so that we achieve local competition in V1 and PP ($\sigma = 8$). It is by introducing this into the model that we can explain object-based neglect and the related effects shown in the figures.

The local lateral inhibitory interactions $I_{ij}^{\text{I,PP}}$ in the PP module in the dorsal stream are given by

$$I_{ij}^{\mathrm{I,PP}} = \sum_{\tilde{i},\tilde{j}} w_{ij\tilde{i}\tilde{j}}^{\mathrm{I,PP}} \mathrm{F}(A_{\tilde{i}\tilde{j}}^{\mathrm{PP}}(t)) \tag{14}$$

$w_{ij\tilde{i}\tilde{j}}^{\mathrm{I,PP}} = 1$ being the lateral local connections between lateral nodes defined by:

$$\begin{cases} w_{ij\tilde{i}\tilde{j}}^{\mathrm{I,PP}} = 1.0 & \text{if } i = \tilde{i} \text{ and } j = \tilde{j} \\ w_{ij\tilde{i}\tilde{j}}^{\mathrm{I,PP}} = -\delta \exp\left\{ -\dfrac{\mathrm{dist}(c_{ij}, c_{\tilde{i},\tilde{j}})^2}{\sigma_{\mathrm{PP}}^2} \right\} & \text{else} \end{cases} \tag{15}$$

In the particular case of PP, the centre c_{ij} coincides with the location ij in the retinal input matrix.

In our simulations, we use $\alpha = 0.95$, $\beta = 0.8$, $\gamma_f = 1$, $\gamma_b = 0.2$, $\lambda_f = 1$, $\lambda_b = 0.2$, $\delta = 0.1$, $I_0 = 0.025$ and the standard deviation of the additive noise ν, $\sigma_\nu = 0.02$.

Let us now describe the damage to the model that can account for object-based visual neglect. The visual neglect can be explained by unilateral damage to the PP module of our cortical architecture. In outline, let us divide the neuronal pools in the PP module into two pools, for the left and right hemispheres. The left (right) hemisphere is associated with the right (left) visual field. A group of neuronal pools in a given module can be impaired in an intrinsic way (Humphreys & Heinke, 1998) by damaging only intrinsic inputs within the module. In mathematical terms, the intrinsic lesioning of a neuronal pool in the PP module is described by extending the PP update equations to:

$$\begin{aligned} \tau \frac{\partial A_{ij}^{PP}(t)}{\partial t} = & -A_{ij}^{\mathrm{PP}} + L_{ij}\{\alpha \mathrm{F}(A_{ij}^{\mathrm{PP}}(t)) - \beta \mathrm{F}(A^{\mathrm{I,PP}}(t)) \\ & + I_0\} + I_{ij}^{\mathrm{PP-V1}}(t) + I_{ij}^{\mathrm{PP,A}} + \nu \end{aligned} \tag{16}$$

where L_{ij} is a lesioning factor (and $I_{ij}^{\mathrm{PP,A}}$ is a spatial attentional bias that was not used in the simulations described here). Values of L_{ij} equal to 1.0 leave the corresponding neuronal pools unaffected, whereas values of L_{ij} smaller than 1.0 damage the corresponding neuronal pools by reducing the influence of the intrinsic inputs A_{ij}^{PP}, $A^{\mathrm{I,PP}}$ and I_0.

The lesion pattern consists of a gradient of impairment across the PP module. The corresponding damage factor is given by

$$L_{ij} = 0.1 + 0.9 \cdot i/N \tag{17}$$

This lesion pattern is designed to model the gradient of impairment in neglect following right parietal cortex damage (Mozer & Behrmann, 1990; Kinsbourne, 1993; Driver, Baylis, Goodrich & Rafal, 1994; Anderson, 1996; Mozer, Halligan & Marshall, 1997; Pouget & Sejnowski, 1997). The response to stimuli is increasingly impaired the further the stimuli are towards the patient's (egocentric) left. The damage factor equation 17 reflects the decreasing number of parietal cells in the lesioned system for positions toward the left in the visual field.

The 2D Gabor wavelet preprocessing

The first step in the preprocessing consists of removing the DC component of the image, i.e. the mean value of the grey-scale intensity of the pixels. (The equivalent in the brain is the low-pass filtering performed by the retinal ganglion cells and lateral geniculate cells. The visual representation in the LGN is essentially a contrast-invariant pixel representation of the image, i.e. each neuron encodes the relative brightness value at one location in visual space referred to the mean value of the image brightness). We denote this contrast-invariant LGN representation by the $N \times N$ matrix Γ_{ij} defined by the equation

$$\Gamma_{ij} = \Gamma_{ij}^{\mathrm{orig}} - \frac{1}{N^2} \sum_{i=1}^{N} \sum_{j=1}^{N} \Gamma_{ij}^{\mathrm{orig}}. \tag{18}$$

Feedforward connections to a layer of V1 neurons perform the extraction of simple features like bars at different locations, orientations and sizes. Realistic receptive fields for V1 neurons that extract these simple features can be represented by 2D-Gabor wavelets. Lee (1996) derived a family of discretized 2D-Gabor wavelets that satisfy the wavelet theory and the neurophysiological constraints for simple cells. They are given by an expression of the form

$$G_{pqkl}(x,y) = a^{-k} \Psi_{\theta_l}(a^{-k}(x-2p), a^{-k}(y-2q)) \tag{19}$$

where

$$\Psi_{\theta_l} = \Psi(x \cos(l\theta_0) + y \sin(l\theta_0), -x \sin(l\theta_0) + y \cos(l\theta_0)) \tag{20}$$

and the mother wavelet is given by

$$\Psi(x,y) = \frac{1}{\sqrt{2\pi}} \mathrm{e}^{-\frac{1}{8}(4x^2+y^2)} [\mathrm{e}^{\kappa i x} - \mathrm{e}^{-\frac{\kappa^2}{2}}]. \tag{21}$$

In the above equations, $\theta_0 = \pi/L$ denotes the step size of each angular rotation, l the index of rotation corresponding to the preferred orientation $\theta_l = l\pi/L$, k the octave, and the indices pq the position of the receptive field centre at $c_x = p(N/N_{\mathrm{V1}})$ and $c_y = q(N/N_{\mathrm{V1}})$. In this form, the receptive fields at all levels cover the spatial domain in the same way, i.e. by always overlapping the receptive fields in the same fashion. In the model we use $a = 2$, $b = 1$ and $\kappa = \pi$, corresponding to a spatial frequency bandwidth of one octave.

The neurons in the pools in V1 have receptive fields that reflect a Gabor wavelet transform performed on the image. Let us denote by I_{pqkl}^{V1} the sensory input activity to a pool A_{pqkl}^{V1} in V1 which is sensitive to a spatial frequency at octave k, to a preferred orientation defined by the rotation index l, and to stimuli at the centre location specified by the indices pq. The sensory input activity to a pool in V1 is therefore defined by the modulus of the convolution between the corresponding receptive fields and the image, i.e.

$$I_{pqkl}^{\mathrm{V1}} = \sqrt{\|\langle G_{pqkl}, \Gamma \rangle\|^2} = \sqrt{\|\sum_{i=1}^{N} \sum_{j=1}^{N} G_{pqkl}(i,j) \Gamma_{ij}\|^2} \tag{22}$$

and is normalized to a maximal saturation value of 0.025.

Abbreviations

IT, inferior temporal cortex; PP, posterior parietal cortex; V1, primary visual cortex.

References

Abbott, L.F. (1991) Realistic synaptic inputs for model neural networks. *Network*, **2**, 245–258.

Amit, D.J. & Tsodyks, M.V. (1991) Quantitative study of attractor neural network retrieving at low spike rates. I. substrate – spikes, rates and neuronal gain. *Network*, **2**, 259–273.

Anderson, B. (1996) A mathematical model of line bisection behaviour in neglect. *Brain*, **119**, 841–850.
Behrmann, M. & Tipper, S.P. (1999) Attention accesses multiple spatial frames of reference: Evidence from neglect. *J. Exp. Psychol. Hum. Percept. Perform.*, **25**, 83–101.
Bisiach, E. (1996) Unilateral neglect and the structure of space representation. *Current Directions Psychol. Sci.*, **5**, 62–65.
Boutsen, L. & Humphreys, G.W. (2002) Axis-based grouping reduces visual extinction. *Neuropsychologia*, **38**, 896–905.
Deco, G. (2001) Biased competition mechanisms for visual attention. In Wermter, S., Austin, J. & Willshaw, D. (eds), *Emergent Neural Computational Architectures Based on Neuroscience*. Springer, Heidelberg, pp. 114–126.
Deco, G., Heinke, D., Zihl, J. & Humphreys, G. (2002) A computational neuroscience account of visual neglect. *Neurocomputing*, **44–46**, 811–816.
Driver, J., Baylis, G.C., Goodrich, S. & Rafal, R. (1994) Axis-based neglect of visual shapes. *Neuropsychologia*, **32**, 1353–1365.
Driver, J. & Pouget, A. (2000) Object-centered visual neglect, or relative egocentric neglect? *J. Cogn. Neurosci.*, **12**, 542–545.
Eglin, M., Robertson, L. & Knight, R. (1989) Visual search performance in the neglect syndrome. *J. Cogn. Neurosci.*, **1**, 372–385.
Gainotti, G., Messerli, P. & Tissot, R. (1972) Qualitative analysis of unilateral spatial neglect in relation to laterality of cerebral lesions. *J. Neurol. Neurosurg. Psychiatry*, **35**, 545–550.
Gerstner, W. (2000) Population dynamics of spiking neurons: Fast transients, asynchronous states, and locking. *Neural Comput.*, **12**, 43–89.
Gilchrist, I., Humphreys, G.W. & Riddoch, M.J. (1996) Grouping and extinction: evidence for low-level modulation of selection. *Cognitive Neuropsychol.*, **13**, 1223–1256.
Humphreys, G.W. & Heinke, D. (1998) Spatial representation and selection in the brain: Neuropsychological and computational constraints. *Visual Cognition*, **5**, 9–47.
Kinsbourne, M. (1993) Orientational bias model of unilateral neglect. Evidence from attentional gradients within hemispace. In Robertson, I. & Marshall, J. (eds), *Unilateral Neglect: Clinical and Experimental Studies.* Erlbaum, Hove, pp. 63–86.
Lee, T.S. (1996) Image representation using 2D Gabor wavelets. *IEEE Trans. Pattern Anal. Machine Intelligence*, **18**, 959–971.
Marshall, J. & Halligan, P. (1993) Visuo-spatial neglect: a new copying test to assess perceptual parsing. *J. Neurol.*, **240**, 37–40.
Mozer, M. & Behrmann, M. (1990) On the interaction of selective attention and lexical knowledge: a connectionist account of neglect dyslexia. *J. Cogn. Neurosci.*, **2**, 96–123.
Mozer, M.C., Halligan, P.W. & Marshall, J.C. (1997) The end of the line for a brain-damaged model of unilateral neglect. *J. Cogn. Neurosci.*, **9**, 171–190.
Posner, M., Walker, J., Friedrich, F. & Rafal, B. (1984) Effects of parietal injury on covert orienting of attention. *J. Neurosci.*, **4**, 1863–1874.
Pouget, A. & Driver, J. (1999) Visual neglect. In Wilson, R. & Keil, F. (eds), *MIT Encyclopedia of Cognitive Sciences*. MIT Press, Cambridge, pp. 869–871.
Pouget, A. & Sejnowski, T. (1997) New view of hemineglect based on the response properties of parietal neurons. *Philos. Trans. R. Soc. Lond. B Biol. Sci.*, **352**, 1449–1459.
Rafal, R. & Robertson, L. (1997) The neurology of visual attention. In Gazzaniga, M. (ed.), *The Cognitive Neuroscience*. MIT Press, Cambridge, pp. 625–648.
Rolls, E.T. & Deco, G. (2002) *Computational Neuroscience of Vision*. Oxford University Press, Oxford.
Rolls, E.T. & Treves, A. (1998) *Neural Networks and Brain Function*. Oxford University Press, Oxford.
Vallar, G. & Pernai, D. (1986) The anatomy of unilateral neglect after right-hemisphere stroke lesions. A clinical/CT-scan correlation study in man. *Neuropsychologia*, **24**, 609–622.
Vuilleumier, P. & Sagiv, N. (2001) Two eyes make a pair: facial organization and perceptual learning reduce visual extinction. *Neuropsychologia*, **39**, 1144–1149.
Wilson, H. & Cowan, J. (1972) Excitatory and inhibitory interactions in localised populations of model neurons. *Biophys. J.*, **12**, 1–24.